

# NUMERICAL MODELING AND EXPERIMENTAL EVALUATION OF AN HIGH-SPEED TRAIN PANTOGRAPH AERODYNAMIC NOISE

D. SIANO<sup>1</sup>, M. VISCARDI<sup>2</sup>, F. DONISI<sup>2</sup>, P. NAPOLITANO<sup>2</sup>

<sup>1</sup> CNR (National Research Council of Italy) - Istituto Motori  
Viale Marconi, 8 – 80125 Naples ITALY  
d.siano@im.cnr.it

<sup>2</sup> Department of Industrial Engineering, University of Naples “Federico II”  
Via Claudio, 21 – 80125 Naples ITALY  
massimo.viscardi@unina.it

*Abstract:* - Several studies to increase train speed are underway with the target to design a new generation pantograph in order to reduce aerodynamic noise. The aerodynamic characteristics as shapes of pantograph are the main issue.

The present work deals with a high-speed aerodynamic and aeroacoustic analysis of a three-dimensional pantograph model, through the employment of 3D numerical simulations. In particular, a computational fluid dynamics-based analysis is performed using commercial software code FLUENT Ansys<sup>TM</sup> and an experimental campaign is performed in the high-speed wind tunnel in order to verify the accuracy of numerical approach. The aerodynamic noise is, then, calculated through the Ffowcs Williams—Hawkings (FW-H) equation to evaluate the flow induced sound pressure level in aeroacoustics. The numerical and experimental results are then compared in terms of sound pressure levels and a well agreement has been found. The numerical results in terms of visualization of pressure distribution on the pantograph provides useful information for pantograph design. The results highlight the possibility to develop a new design of the pantograph for high-speed trains, in order to obtain an aerodynamic noise reduction.

*Keywords:* Radiated Noise, 3D CFD analysis, Aeroacoustic, Aerodynamic, Pantograph.

## 1 Introduction

In recent years major advances have been made in the ability to calculate fluid flows using computational fluid dynamics (CFD) and these can be used to optimize a vehicle for aerodynamic performance (e.g. aerodynamic drag). Nevertheless, there is a large step between such calculations and predictions of aerodynamic noise (computational aero-acoustics, CAA). In general, most applications of CAA have been limited to special cases of limited geometry and practical application to industrial geometry is less common. Nevertheless, there are various numerical approaches that can be taken in

account to estimate the aerodynamic noise, some of which have been used to study railway applications. As a general consideration it can be stated that when the maximum speed of high-speed trains reaches 320 km/h, the performance of pantographs is strongly influenced by the effects of aerodynamics. Indeed, aero-acoustic noise generated by pantographs during high-speed running has become one of the main noise sources on such trains. This contribution very often become the main noise source that needs to be reduced to fulfill with the environmental standard that limit the wayside noise of high-speed trains. There is therefore a strong demand for reductions in the aerodynamic noise of the pantograph to decrease

wayside noise, and continuous efforts toward this goal have brought about the evolution of a low-noise pantograph.

The objective of the present study is to verify the performance of CFD numerical approach in order to get useful information on subsystems design optimization to reduce its aerodynamic noise. The results reported here highlight the possibility to improve the shapes of such structures in order to obtain a significantly noise reduction.

The activity, based on the availability of experimental data on the SSS87 pantograph, has been focused on the development of relative CAA model and data comparison.

This preliminary activity is involved within a more complex activity of design and noise prediction for a new high speed pantograph, but has represented a very important activity, as permitted the validation of the proposed numerical approach.

## 2 Reference experimental data

The reference data used inside this activity, derived from a previous detailed study included in an European project contest.

Experimental acoustic measurements have been performed on the pantograph model SSS 87 in the Deutsch-Niederlandischen Windkanal (DNW) (Germany) wind tunnel to analyze aerodynamic noise emission [4], [5]. More precisely:

- The pantograph was placed on a fixed metal sheet, flushed with the nozzle lower edge, and positioned at 3.43m from the wind tunnel nozzle output section (see figure 1),
- The pantograph was tested in its mean working condition (approximately opened at 1.6m from the train roof),
- Experimental tests were conducted at different flow speeds: 32m/s, 48m/s, 64m/s, 78m/s,
- A B&K microphones array (vertical antenna) was placed at a distance of 4.89m from the pantograph symmetry plane.

Fig.1 shows a sketch of the experimental test apparatus. Maximum wind speed was about 78m/s with a turbulence intensity being less than 0.2%.

As a result of the experimental tests in all above mentioned flow conditions, the time-domain signal

of each microphone was acquired. The SPL in frequency domain with a frequency resolution of 11.6Hz, was then acquired.

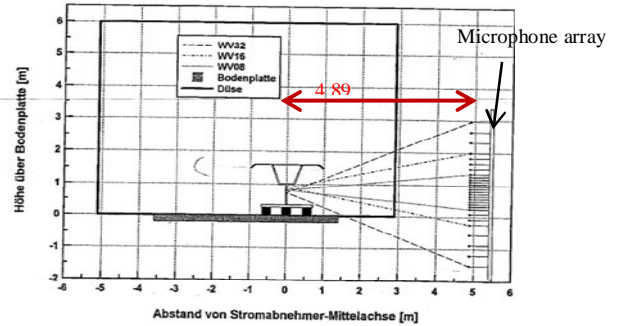


Fig. 1: experimental wind tunnel test apparatus

A summary of the measured results, is reported in next Fig.2, where the experimental overall SPL at different operating speed conditions are shown.

It has to be noted that the curves show similar trends, even if overall translated with reference to the flow velocity. They present a descendent behavior of about 10 dB in the 100-1000 Hz frequency range. A more noise abatement of about 20 dB is present in the 1-5 kHz frequency range. A noise peak at approximately 250Hz is more evident in the 78 m/s speed condition.

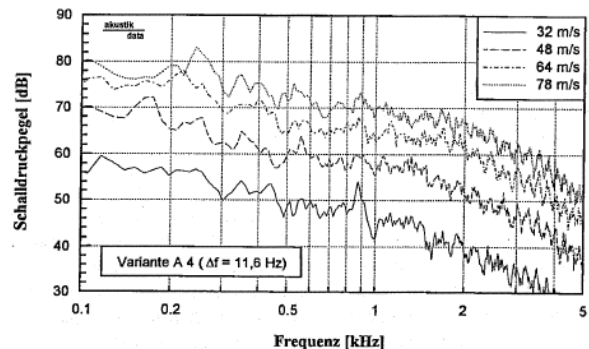


Fig. 1: experimental pantograph aerodynamic noise SPL (dB)

In Fig.3, the equivalent SPL expressed in dB(A) between 100Hz and 5 kHz, at different train speeds are reported.

| 32 m/s<br>[dB(A)] | 48 m/s<br>[dB(A)] | 64 m/s<br>[dB(A)] | 78 m/s<br>[dB(A)] |
|-------------------|-------------------|-------------------|-------------------|
| 71,0              | 82,8              | 90,9              | 96,3              |

Fig.2: experimental overall SPL dB(A)

### 3 CAA analysis

In order to numerically compute the acoustic emission of the pantograph SSS 87, several steps have been executed for building up and then analyze the numerical model: starting from a 2D drafting, a 3D CAD model of the fluid control volume around the structure has been created and then meshed and analyzed according to defined boundary conditions.

Because of experimental results demonstrated a similar trend of the SPL curves at different train speeds, the CAA analysis of the pantograph have been run in the highest speed condition (78m/s), corresponding to the noisiest operating condition, also to reduce the calculations time.

#### 3.1 geometrical design

In this paragraph, a description of the design procedure is reported.

Because there was only a 2D pantograph design model, a 3D CAD model of the pantograph SSS 87 has been built using the software CATIA V5® (Fig.4). Considering the purpose of the model, it has been built up very carefully:

- In order to simplify the meshing operation and the computer solving time, small features of the pantograph, such as screws, cables or holes, have been neglected.
- Considering the maximum frequency measured during the experimental analysis (5 kHz), small components of the structure has been neglected
- The pantograph in the 2D drafting is in its “sleeping” condition; in order to compare the numerical simulation with the experimental ones, it has been necessary to develop the 3D model in its mean working condition.

Once the 3D pantograph CAD model has been designed, the surrounding fluid control volume has been created.

Specifically, a cylindrical control volume, length of 3.8m and a diameter of 3m, is realized.

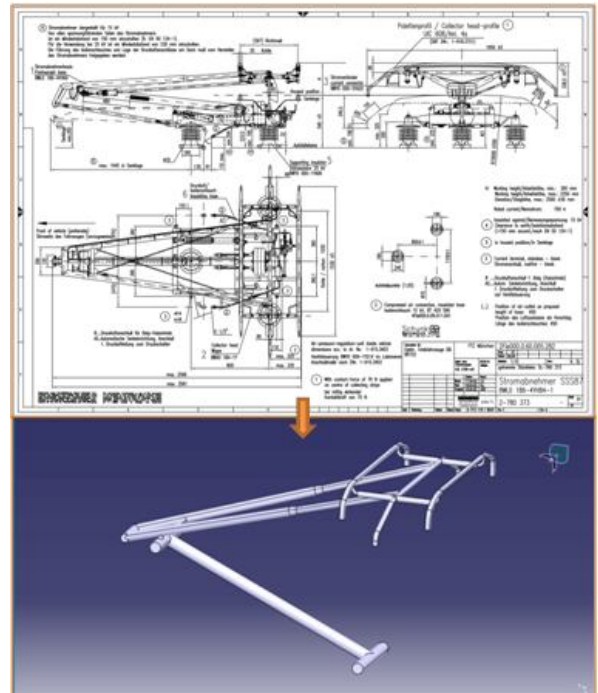


Fig.4: 3D CAD model obtained after 2D manipulation

In order to simplify the model and reduce the computing time a symmetry plane of the pantograph was considered.

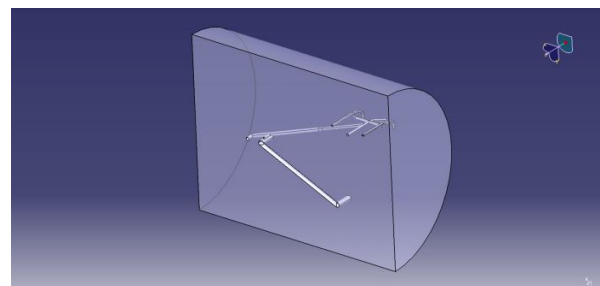


Fig.5: fluid control volume around the object

The mesh process represents an important operation to achieve with good accuracy numerical results. For this reason, the mesh has been realized finer close to the wall boundaries and around the object to study, in order to take into account the viscous effects inside the boundary layer. Far away from the body the flow is undisturbed, so the mesh can be coarser. According to the acoustic analysis, the mesh has to be fine enough in the entire fluid volume in order to allow the sound wave propagation. The maximum element dimension has to be considered not greater than 1/5 of the considered wavelength.

Fig.6 and Fig.7 show the entire volume and a zoom of the realized mesh model, respectively.

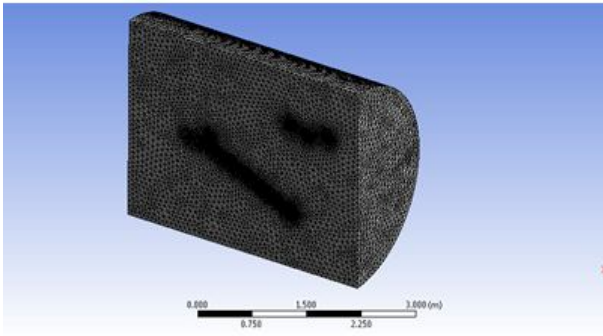


Fig.6: control volume mesh

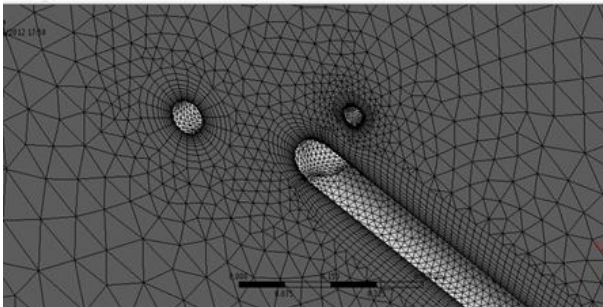


Fig.7: detailed control volume mesh

For the purpose of the analysis tetrahedrons elements have been chosen. The maximum length of element's edge is approximately 0.04m (according to the acoustic analysis requirements). Because of, the pantograph surfaces represent wall boundaries, the mesh has been thickened in their proximities, using a transition ratio during the inflation process of 0.5 (it means that in the proximity of a wall, the elements will halve their dimensions).

### 3.2 analysis conditions

FLUENT solver with the k- $\epsilon$  realizable simulation model, characterizing non-stationary phenomena such as vortex shedding, three-dimensional flow field was used for calculations [3]. Table 2 shows the applied characteristics for computational domain. The no-slip condition for velocity is applied to the model surface. The outlet is set to an outflow boundary condition, which dictates a zero diffusion flux.

Specifically:

- A transient analysis is realized in order to take into account vortex shedding phenomena,

- The used turbulence model is the k- $\epsilon$  realizable;
- Both the “Time step” and “Number of time steps” parameters have been set according to acoustics requirements; in fact, the time step determines the highest frequency that can be measured on the basis of the Nyquist-Shannon sampling theorem, [5], and the the frequency resolution of the signal.

|                             |                             |
|-----------------------------|-----------------------------|
| Type of analysis            | Transient, pressure-based   |
| Fluid dynamic model         | k- $\epsilon$ realizable    |
| Wall conditions             | Standard wall function      |
| Inlet boundary condition    | Uniform velocity (78 m/s)   |
| Outlet boundary condition   | Uniform pressure            |
| External surface condition  | Wall with 0m RH             |
| Object surface condition    | Wall with 1e-3m RH          |
| Residual values             | 1e-5                        |
| Aero Acoustics model        | Ffwoocs Williams - Hawkings |
| Sound source                | Body surface                |
| Number of receivers         | 35                          |
| Time step                   | 2,5e-4 s                    |
| Number of time steps        | 400                         |
| Max iteration per time step | 300                         |

Table 1: CAA Analysis settings

Fig.8 reports the simulated microphone array replying perfectly the experimental position. The array was composed of 35 microphone receivers at a distance of 0.4 m from each other (width 2.4 m and height 1.6 m).

In order to simulate the acoustic far field condition, the microphones array has been set at a distance 1m from the pantograph's symmetry plane.

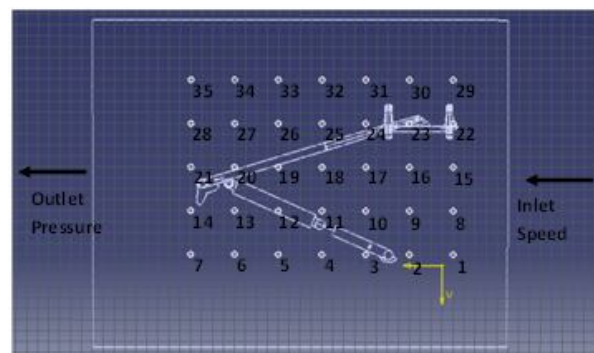


Fig.8: numerical receivers array

A set of computational tests have been performed in order to verify the robustness and reliability of the model:



- **Robustness check:** three different mesh models have been realized in order to verify the goodness of the results.
- **Speed Sensitivity check:** the aim of the test is to verify that the model was stable. Three different speeds have been chosen: 77m/s, 78m/s and 79m/s. The results have proven that the output of the system does not change significantly.

### 3.3 Results

In Fig.9, the instantaneous fluid flow around the pantograph is shown; the flow field has a highly 3D behavior, starting from a uniform condition of 78m/s (applied normal to the inlet surface), the fluid shows an acceleration in proximity of the object and some turbulent wakes behind it are present. In fact, the fluid separates on the sides of the object and the streamlines cannot follow its profile until the end of it, generating low pressure and turbulent regions.

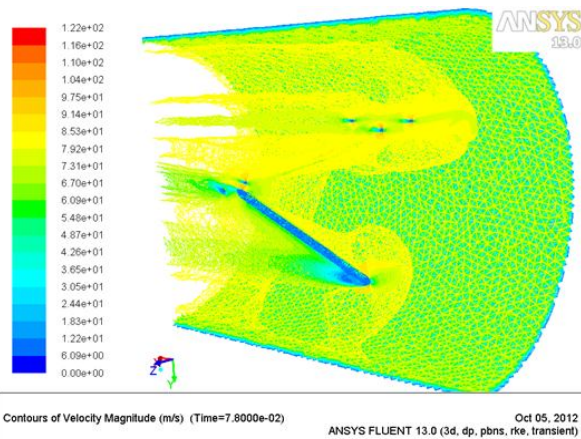


Fig.9: instantaneous numerical contours of velocity around the pantograph

Looking at the evolution of the flow through time, it is interesting to notice that despite the uniform and stationary inlet condition, the flow field inside the control volume evolves through time: this is due to the fact that turbulent flows are highly non stationary phenomena.

Unfortunately, due to the turbulent model used, after a first non-stationary time interval, the flow tends to become stationary: looking at the evolution of the acoustic pressure during the acquisition time at a fixed receiver (Fig), it is evident that after a first period of transient signal, the pressure becomes stationary for approximately 0.05s (half of the

sampling time); this means that after 0.05s, the flow in the control volume becomes stationary.

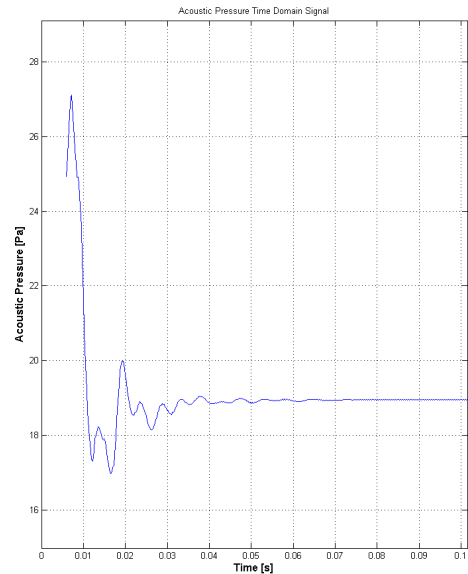


Fig.10: acoustic Pressure vs. Time at receiver

Analyzing a signal composed of a non-stationary part and a stationary one, will give back wrong results. The reason is that an acoustic occurrence has to be measured with a microphone, but analyzing a signal as the one in Fig. 10 is like measuring the desired acoustic occurrence and continuing the measure even after the phenomenon ends. This procedure is obviously wrong and so, in order to have realistic results, is correct to analyze only the non-stationary part of the signal (the actual acoustic phenomenon). In order to realize this, the “Pressure VS Time” signal has been trimmed at 0.05s, so that the acoustic post-processing is computed only on the non-stationary part of the phenomenon.

As done in the experimental post-processing, the pressure at the receivers have been averaged.

In Fig. 11, the numerical and experimental mean SPL emitted by the pantograph between 100Hz and 2000Hz are shown. The frequency behavior of the numerical model strictly follow the experimental one; the numerical simulation has been able to reproduce almost every single noise peak detected in the experimentation with just a slight frequency gap between experimental and numerical peaks due to the different frequency resolution used.

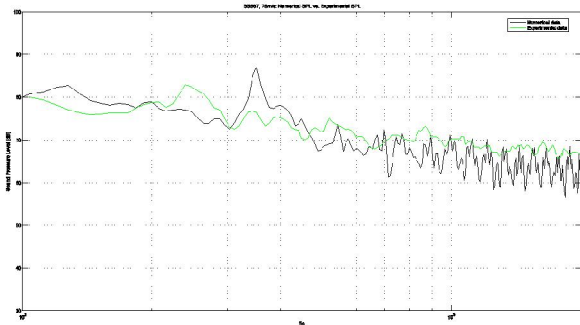


Fig.11 : numerical and Experimental SPL frequency spectrum at 78m/s

In table 2, the SPL Overall value at different train speed is shown; in order to read the values in the table, it is important to do the following assumptions:

- The numerical simulation has been performed at flow speed of 78m/s, while the numerical values at 64m/s and 48m/s are the results of an analytical manipulation of the SPL, considering the SPL variation with speed given by the experimental results.
- The numerical simulation has been capable of generating an SPL up to 2kHz, while the experimental analysis has gone up to 5kHz; the experimental SPL Overall values have been calculated between 100Hz and 5kHz, while the numerical SPL Overall values have been calculated between 100Hz and 2kHz; that is the reason why the numerical and experimental SPL Overall values presents some differences.

| SPL Overall Value<br>dB(A) |       |       |           |       |       |
|----------------------------|-------|-------|-----------|-------|-------|
| Experimental               |       |       | Numerical |       |       |
| 48m/s                      | 64m/s | 78m/s | 48m/s     | 64m/s | 78m/s |
| 82.80                      | 90.90 | 96.30 | 79.94     | 86.11 | 92.32 |

Table 2: comparison between experimental and numerical Overall SPL at different speeds

Moreover, by the use of the numerical simulation, the regions of the object causing more noise have been detected. It has been, in fact, discovered that the regions that generate more noise are the central part of the arc and the junction between the trapezium and the arm (the knee, evidenced in Fig.12), these are the same results found during the SSS 87 experimental simulations.

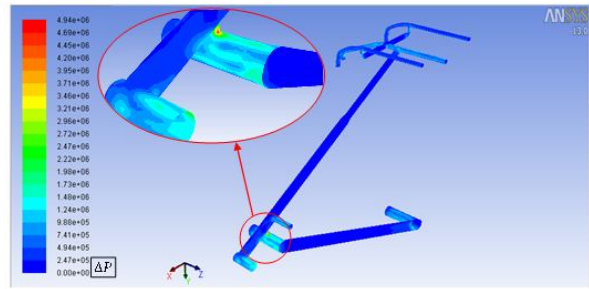


Fig.12: numerical noise emission power contour map on the pantograph

## 4 Conclusions

As a general conclusion of the activity, it can be stated that numerical model for the prediction of high-speed train pantograph's aerodynamic noise has been developed.

The numerical model strictly reproduces the real sound pressure level spectrum emitted by the pantograph.

Through the use of the numerical model it is possible to detect the part of the pantograph generating more noise.

For these reasons it can be said that the aerodynamic noise prediction method developed is efficient, reliable and accurate. The method will so used for the prediction of aerodynamic noise emission for a similar high speed train pantograph system.

Already ongoing activities, will develop furthermore the method and will also include:

- the implementation of an analytical formulation approach that will permit fast but reliable pre-design evaluation
- a noise optimization tool to geometrically optimize the most radiating area, in order to reduce the overall emitted noise.

## References

[1] Smith M.G., Chow L.C., *Prediction Method for Aerodynamic Noise from Aircraft Landing Gears*, AIAA 98-2228

[2] Lighthill M.J.: *On sound generated aerodynamically. I. General theory*, Proceedings of the Royal Society of London. Series A, Mathematical and Physical Sciences 211(1107), 564–587 (1952)

[3] Ffowcs Williams J. E., Hawkins D. L., *Sound generated by turbulence and surfaces in arbitrary*

*motion*, London: Philosophical Transactions of the Royal Society of London, (1969)

[4] Ingenieurbüro akustik-data, Dipl.-Ing. B. Barsikow, *Bestimmung der Schallemission verschiedener Varianten des Stromabnehmers SSS 87 im Deutsch-Niederländischen Windkanal (DNW)*, Bericht Nr. 97/2, Kirchblick 9 D-14129 Berlin, (1997)

[5] Viscardi M., Rusciano N., Iadevaia M. & Siano D., *An optimization process experience for HVAC noise emission and flows distribution inside a passenger's train wagon*, 16th International Congress on Sound and Vibration 2009, ICSV 2009, pp. 3334.(2009)

[6] Shannon C. E., *Communication in the presence of noise*, Proc. Institute of Radio Engineers, vol. 37, no. 1, (1949)